ENVIRONMENTAL RESEARCH
LETTERS

LETTER • OPEN ACCESS

Drivers of exceptionally cold North Atlantic Ocean temperatures and their link to the 2015 European heat wave

To cite this article: Aurélie Duchez *et al* 2016 *Environ. Res. Lett.* **11** 074004

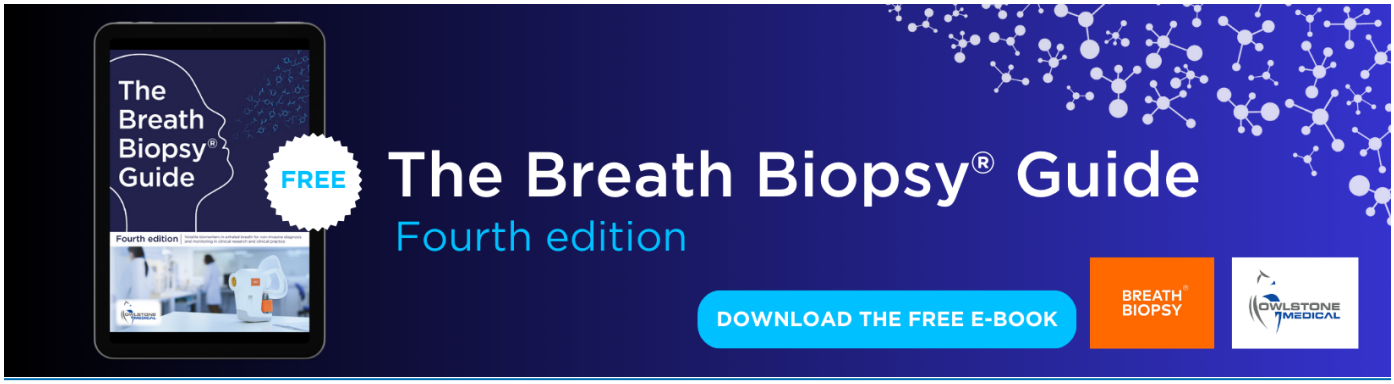

Environmental Research Letters

LETTER

Drivers of exceptionally cold North Atlantic Ocean temperatures and their link to the 2015 European heat wave

Aurélie Duchez[1,3], **Eleanor Frajka-Williams**[2], **Simon A Josey**[1], **Dafydd G Evans**[2], **Jeremy P Grist**[1], **Robert Marsh**[2], **Gerard D McCarthy**[1], **Bablu Sinha**[1], **David I Berry**[1] **and Joël J-M Hirschi**[1]

[1] National Oceanography Centre, University of Southampton Waterfront Campus, European Way, Southampton SO14 3ZH, UK
[2] Ocean and Earth Science, National Oceanography Centre, University of Southampton Waterfront Campus, European Way, Southampton SO14 3ZH, UK
[3] Author to whom any correspondence should be addressed.

E-mail: aurelie.duchez@noc.ac.uk

Keywords: 2015 heat wave, cold Atlantic Ocean anomaly, ocean atmosphere interactions, North Atlantic, ocean variability, air-sea fluxes

Supplementary material for this article is available online

OPEN ACCESS

RECEIVED
16 February 2016

REVISED
11 May 2016

ACCEPTED FOR PUBLICATION
14 June 2016

PUBLISHED
5 July 2016

Abstract

The North Atlantic and Europe experienced two extreme climate events in 2015: exceptionally cold ocean surface temperatures and a summer heat wave ranked in the top ten over the past 65 years. Here, we show that the cold ocean temperatures were the most extreme in the modern record over much of the mid-high latitude North-East Atlantic. Further, by considering surface heat loss, ocean heat content and wind driven upwelling we explain for the first time the genesis of this cold ocean anomaly. We find that it is primarily due to extreme ocean heat loss driven by atmospheric circulation changes in the preceding two winters combined with the re-emergence of cold ocean water masses. Furthermore, we reveal that a similar cold Atlantic anomaly was also present prior to the most extreme European heat waves since the 1980s indicating that it is a common factor in the development of these events. For the specific case of 2015, we show that the ocean anomaly is linked to a stationary position of the Jet Stream that favours the development of high surface temperatures over Central Europe during the heat wave. Our study calls for an urgent assessment of the impact of ocean drivers on major European summer temperature extremes in order to provide better advance warning measures of these high societal impact events.

1. Introduction

The North Atlantic-Europe region experienced a striking juxtaposition of temperature extremes in 2015 with exceptionally cold ocean surface temperatures developing in the first half of the year and a major heat wave over Central Europe in the summer that followed (figure 1(a)). The causes of both of these events are outstanding research questions. In this paper, we determine for the first time the causes of the 2015 cold ocean anomaly. Additionally, we find a relationship between ocean temperatures and European heat waves since 1980, including the one in 2015, which indicates that cold mid-latitude ocean temperature anomalies are a common precursor to heat wave events and need to be included amongst their potential drivers.

The outstanding problem in understanding European heat waves is a reliable identification of the factors that cause them to develop (Perkins 2015). Several regional drivers have been put forward including soil moisture, precipitation deficits and anomalously warm surface temperatures in marginal seas particularly the Mediterranean (Vautard *et al* 2005, Fischer *et al* 2007, Feudale and Shukla 2011a, Stefanon *et al* 2012). Another factor is the North Atlantic Ocean as it has the potential to modify the atmospheric circulation upstream of Europe prior to the development of a heat wave through the influence of anomalies in the temperature of the sea surface (e.g. Brayshaw *et al* 2011, Dong *et al* 2013, Buchan *et al* 2014). This precursor role for the Atlantic has received little attention to date although previous studies have found some evidence for the influence of sea surface

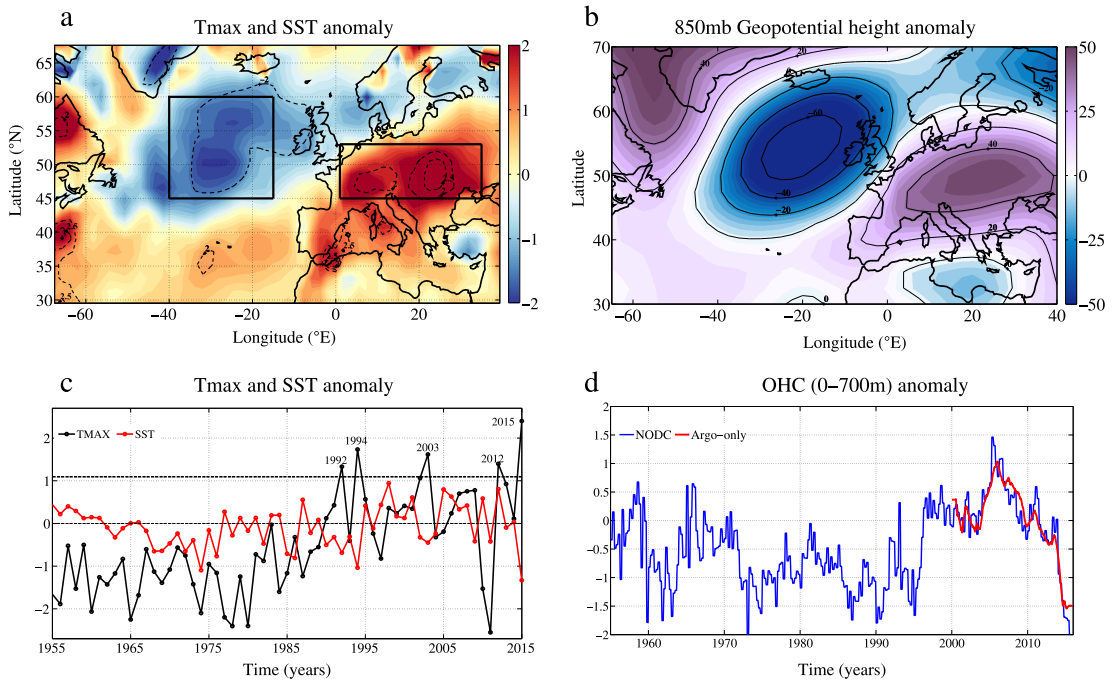

Figure 1. (a) 2015 JJA sea surface temperature anomalies (over the ocean) and maximum 2 m air temperature anomalies (over land) in °C (shading). Contours delineate regions exceeding 2 and 2.5 standard deviations (contours). The left box indicates the area chosen to define the cold Atlantic SST anomaly; the right box indicates the area used to define the maximum 2 m air temperature anomaly. (b) Anomalies of geopotential height (in m) at 850 mb for JJA 2015. (c) Evolution of JJA SST anomalies (red, averaged over left box) and maximum 2 m air temperature anomalies (black, averaged over right box). The seasonal cycle for 1981–2010 has been removed. (d) Ocean heat content anomaly time series (in GJ m^{-2}) up to Dec 2015 averaged over the box (45°–60°N, 40°–15°W) and extracted from the National Oceanographic Data Center (NODC) 0–700 m product (blue). Argo profiles represent the main source of data after 2003, as shown by an Argo-only index smoothed with a 12 month running window (red). Both time series are referenced to the period 2000–2015 and show a stronger reduction since 2013.

temperature (SST) anomalies acting at the same time as the heat wave (Black *et al* 2004, Nakamura *et al* 2005, Della-Marta *et al* 2007). In addition, a role for atmospheric temperature anomalies over the Tropical Atlantic was found by (Cassou *et al* 2005) although their study did not consider ocean temperature anomalies.

We discuss the data and methods used for our analysis in section 2 and determine the causes of the 2015 North Atlantic cold anomaly in section 3. In section 4, we explore the relationship between North Atlantic Ocean temperature anomalies and European heat waves with an emphasis on the potential role of ocean temperature anomalies as a precursor.

2. Data and methods

Data used in this paper were extracted for the period January 1948–December 2015. The anomalies were calculated by removing the seasonal cycle from January 1981 to December 2010, which is a reference period commonly used by weather services worldwide to define climatological anomalies. The NCEP-NCAR reanalysis (Kalnay *et al* 1996) was used to provide (monthly and daily) SST and monthly 2 m maximum air temperature over Europe, monthly net air–sea heat flux, monthly 850 mb geopotential height and 300 mb zonal wind speed (for the Jet Stream). Output from the ERA-Interim reanalysis (Dee *et al* 2011) has also been used to support the NCEP/NCAR based evaluation of the causes of the cold SST anomaly (see supplementary materials).

Ocean heat content for the time series in figure 1(d) is a monthly product from the National Oceanographic Data Center 0–700 m product. It is derived from profiles in the World Ocean Database (Boyer *et al* 2013). Temperature profiles for the volumetric analysis are from the Roemmich and Gilson Argo climatology, and are available monthly through December 2015 (Roemmich and Gilson 2009). The box chosen for the Atlantic SST anomaly is: 45°N–60°N, 40°W–15°W. We have assessed the sensitivity of our results to the choice of the boxed region for the ocean cold anomaly and found that between 1955 and 2015 changes in ocean heat content and SST mainly occur in this region. For alternative North Atlantic boxes, which encompass the boxed area shown in figure 1(a), our results do not change significantly (not shown). The Central European box chosen to estimate the heat wave temperature is 45°N–53°N, 1°E–35°E.

Variations in SST are governed by the heat balance in the surface mixed layer of the ocean, which is influenced by surface air–sea heat fluxes (influenced by wind speed, air temperature, cloudiness and humidity), horizontal advective and diffusive processes in the

mixed layer, and entrainment processes at the base of the mixed layer. The heat budget for the upper-ocean mixed layer may be written as (Deser *et al* 2010)

$$\frac{dT}{dt} = \frac{Q_{net}}{\rho C_p H} + (\overrightarrow{U_{geo}} + \overrightarrow{U_{ek}}) \cdot \vec{\nabla} T + \frac{(W_e + W_{ek})(T - T_b)}{H}. \quad (1)$$

The first right-hand term in this equation represents the surface heat flux, the second term the horizontal temperature advection, and the last term the vertical water exchange. ρ (1027 kg m^{-3}) is the density of seawater, C_p (3985 J kg^{-1} K^{-1}), the specific heat capacity of seawater, H, the mixed layer depth, T, the mixed layer temperature (equal to the SST), Q_{net}, the net surface heat flux, $U_{geo,}$ the geostrophic current velocity, U_{ek}, the Ekman current velocity, W_e, the vertical entrainment rate, W_{ek}, the Ekman pumping velocity and T_b is the temperature of the water at depth that is entrained into the mixed layer.

Q_{net} is defined as the sum of the sensible and latent (turbulent) heat fluxes and solar and longwave radiative fluxes. The turbulent energy flux is proportional to the wind speed and the sea–air temperature (or humidity) difference, the radiative fluxes are functions of solar elevation, air temperature, humidity and cloudiness. Ekman and geostrophic currents contribute to the heat budget of the mixed layer through horizontal advection, whereas entrainment and Ekman pumping alter the SST through vertical advection. A complete discussion of these terms may be found in texts such as Pond and Pickard (1983) and Vallis (2006), with detailed discussion of the surface fluxes in Josey *et al* (2013). In order to explain the origin of the 2015 cold ocean anomaly, we assess the respective contribution of surface air–sea fluxes, ocean circulation changes (horizontal temperature advection) and vertical water exchange (Ekman upwelling) in section 3.

3. Exceptionally cold North Atlantic in 2015

First, we consider the exceptionally cold ocean surface anomaly that was already in place prior to the onset of the 2015 heat wave. The SST anomaly field for June 2015 (figure 2(a)) shows temperatures up to 2 °C colder than normal over much of the sub-polar gyre with values that are the coldest observed for this month of the year in the period 1948–2015 indicated by stippling. The cause of this cold anomaly has been the subject of widespread interest in the media, we now show for the first time that it can be attributed to a combination of air–sea heat loss from late 2014 through to spring 2015 and a re-emergent subsurface ocean heat content anomaly that developed in preceding years. Prior to the winter of 2014–15, in November 2014, a localised cold SST feature was already evident centred at 50°N, 30°W (figure 2(b)). The subsequent net air-sea heat exchange from December 2014 to May 2015 (figure 2(c)) is characterised by extreme, basin-wide heat loss in the band from 55°–65°N resulting from wind speed anomalies associated with intensification of the meridional surface pressure gradient.

We have determined the June 2015 SST anomaly that is expected from air–sea fluxes by taking the November 2014 SST field as an initial state and adding the December 2014–May 2015 integrated surface heat flux forced SST anomaly using net heat flux from the NCEP/NCAR reanalysis. For the heat flux calculation, a fixed value for the ocean mixed layer depth of 100 m is adopted which is close to the mean value for the box in figure 1(a) for this period. A more detailed calculation would employ time varying MLD but our aim is to show the potential magnitude of the heat flux related signal, for which a fixed value of the MLD over the period is adequate.

The resulting field (figure 2(d)) is in reasonable agreement with the observed SST anomaly (figure 2(a)) particularly in the eastern subpolar gyre. Thus, the extremely cold surface feature can be largely explained in terms of the pre-existing November 2014 SST anomaly and the integrated effects of subsequent surface heat loss from December 2014 to May 2015. A quantitative measure of the level of agreement between the estimated (figure 2(d)) and observed fields (figure 2(a)) is provided by a spatial correlation coefficient value of 0.77 over the domain (35°N–63°N, 40°W–10°W) that spans the key features of the anomaly field. Note that the estimated anomalies are not as strong as those observed on the southern margin of the cold feature, most noticeably in the small region 20–30°W, 45–50°N. This could be due to both the simple assumption of a constant mixed layer depth as well as to the absence of possible contributing effects from the ocean circulation (e.g. changes in the strength of the AMOC and/or of the subpolar gyre).

We have repeated the calculation of the estimated SST anomaly using net heat flux and SST data from the ERA-Interim reanalysis (figure S1 in supplementary materials) and again find close agreement between the estimated and observed SST field in June 2015 indicating that our conclusions are not sensitive to the choice of heat flux product employed.

The anomalous SST in November 2014 is a re-emergence of a cold, subsurface anomaly originating in the winter of 2013–14 (Grist *et al* 2015). Profiles of temperatures in the Atlantic show that the cold anomaly became noticeable in early 2014 and was persistent and intense, representing an average cooling of 0.7 °C throughout the top 700 m in 2015 (figure 3(a)). Some apparent cooling may result from adiabatic heave (upwelling or downwelling of waters). To remove this potential effect, we consider only the volume of water above the 27.6 kg m^{-3} isopycnal (Walin 1982). By considering the variability of volume in each temperature class, we can determine the amount of water that

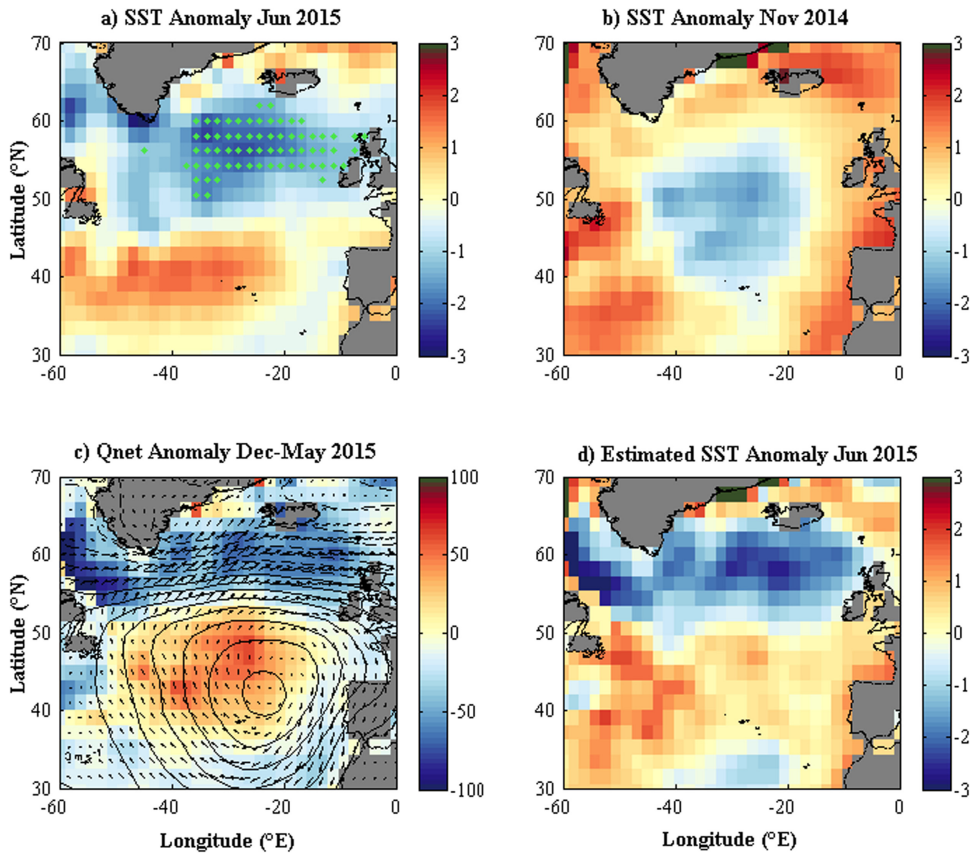

Figure 2. (a) Observed SST anomaly in June 2015, stippled cells indicate that the June 2015 SST is the coldest in that month over the period 1948–2015 (b) observed SST anomaly in November 2014, (c) average net heat flux anomaly for December 2014–May 2015, with corresponding SLP anomaly (contoured, 1 mb intervals, solid lines for positive and zero, dashed lines for negative contours respectively) and 10 m wind speed anomaly (arrows), (d) estimated SST anomaly in June 2015 obtained by integrating the heat flux anomaly in (b) over the ocean mixed layer and adding to the November 2014 initial state in (c). Units are °C for SST and Wm^{-2} for net heat flux.

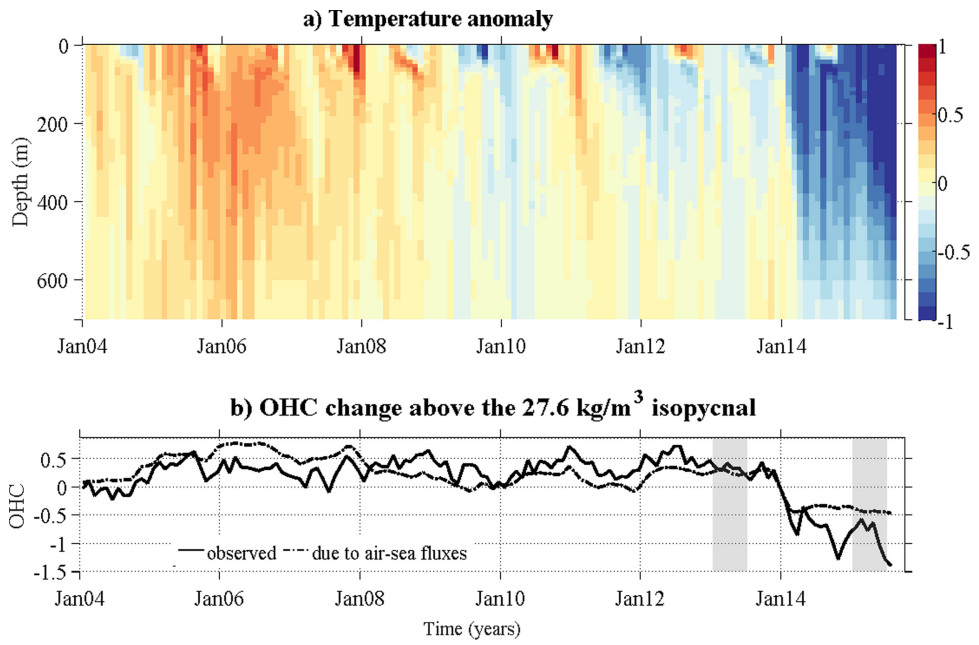

Figure 3. (a) Temperature anomaly in the subpolar gyre (45–60°N, 40–15°W). (b) Observed ocean heat content (OHC) change (in GJ m^{-2}) since 2004 for the volume of water above the 27.6 kg m^{-3} isopycnal. Changes predicted from surface fluxes for the same temperature classes are in dashed. Grey shading highlights the January–June periods in 2013 and 2015. Anomalies in these timeseries were calculated by subtracting the climatology (the background monthly time series) from January 2004 through December 2013.

becomes warmer or cooler and compare that to the warming or cooling predicted by air–sea heat fluxes acting over the same region (figure 3(b)). The volumetric distribution in temperature classes is determined following Marshall *et al* (1993) and Evans *et al* (2014) by summing the total volume of grid cells that lie within each 0.5 °C temperature class using an Argo-based gridded climatology (Roemmich and Gilson 2009, Boyer *et al* 2013). Transformations of water across surfaces of constant temperature (isotherms) are determined by building a series of linear equations describing the volume change in each temperature class in terms of the unknown transformations and solving using a matrix inversion (Evans *et al* 2014). These transformations have units of $m^3\,s^{-1}$. The transformations of water across isotherms predicted by air–sea heat fluxes are determined by integrating the air–sea fluxes over the surface area of the ocean occupied by a specific temperature class. Full details of this method can be found in (Evans *et al* 2014). For this region, the anomalous transformations are then integrated over the volume of water shallower than the 27.6 $kg\,m^{-3}$ isopycnal and accumulated in time, and scaled by density and specific heat capacity to give units of heat content. The monthly mean (using the period from 2004 to the end of 2013) is removed from the time series.

Between January–June 2013 and January–June 2015, the observed cooling of the volume of water represents an OHC change of 1.1 $GJ\,m^{-2}$, with the strongest changes occurring between December 2013 and January 2014 (figure 3(b)). Such a change can either occur through a transformation of water masses by air–sea heat fluxes, or via a net increase in the lateral input of water into colder temperature classes. Estimating the expected OHC change due to air-sea heat fluxes between these same time periods accounts for 0.7 $GJ\,m^{-2}$.

We have also determined the respective contribution from wind driven upwelling (third term in equation (1)) and ocean circulation changes (second term in equation (1)) and found them to be minor terms over this period as we now discuss. Entrainment of relatively cool water from below the mixed layer is associated with upwelling across the subpolar gyre (Marshall *et al* 1993). Fields of monthly upwelling rate were computed from the wind stress curl over the box chosen for the Atlantic SST anomaly. While upwelling was more intense than usual, the associated heat content reduction of 0.2 $GJ\,m^{-2}$ (estimated by multiplying upwelling by the vertical temperature gradient between the surface and 700 m) was only a small proportion of the observed 1.1 $GJ\,m^{-2}$ cooling. Under typical conditions, surface heat losses in the subpolar regions are balanced by the influx of warm subtropical waters carried by the ocean circulation. During the July 2013–June 2015 period, the observed overturning circulation at 41°N, determined using *in situ* floats and satellite altimeters (Willis 2010) was weaker than usual (12.3 Sv compared to 13.6 Sv over the preceding 10 year period), bringing less heat northward. However, the reduced northward flow across 41°N is insufficient to explain the observed heat content changes, nor the observed changes in volumes of water in different temperature classes.

In contrast to the behaviour observed in 2015, circulation changes are thought to be important for the multidecadal to centennial timescale cooling of the North Atlantic evident in analysis of temperature trends over the 20th century (Drijfhout *et al* 2012, Rahmstorf *et al* 2015). On these timescales, an Atlantic warming hole (offset to the south–west from the 2015 anomaly) has been identified. This cooling has been linked to a potential decline in the AMOC (Drijfhout *et al* 2012, Smeed *et al* 2014, Rahmstorf *et al* 2015) and also to the effect of the Atlantic Multi-decadal Oscillation which in recent years has been changing from a positive (anomalously warm North Atlantic) to a negative phase (McCarthy *et al* 2015, Parker and Ollier 2016). It is important to distinguish between this long-term warming hole and the short-term 2015 cold anomaly that is the focus of our study.

4. The 2015 summer heat wave

In the summer of 2015 following the development of the cold ocean anomaly, Europe experienced a major heat wave that has been ranked in the top ten over the past 65 years (Russo *et al* 2015). As pointed out by Meehl and Tebaldi 2004 and Perkins and Alexander 2012, there is no universal definition for heat waves. The heat waves we consider in this study are defined as the summers (JJA) during which the highest 2 m maximum air temperatures were recorded over central Europe in the area shown in figure 1(a).

We now explore whether the development of the 2015 heat wave could have been driven in part by the cold ocean temperatures that preceded it. First we consider the circulation pattern associated with the heat wave. The high temperatures coincided with persistent high and low-pressure systems over Europe and the central North Atlantic respectively (figure 1(b)). This atmospheric pressure pattern subjected Central Europe to the influence of subtropical air masses. Combined with high pressure and summer insolation, this led to the elevated surface air temperatures that were characteristic of the heat wave (figure 1(a)). Using NCEP maximum 2 m air temperatures averaged over Central Europe (defined as the land box in figure 1(a)), we found that the standard deviation (STD) of Tmax from the 1981–2010 mean is 1.1 °C over the 1948–2015 period. The Tmax anomaly for summer 2015 is 2.4 °C, which means that averaged temperatures during that summer were 2.2 STD higher than the mean Tmax summer value for the 1981–2010 period. For the summer of 2003, the Tmax anomaly over our chosen region corresponds to a

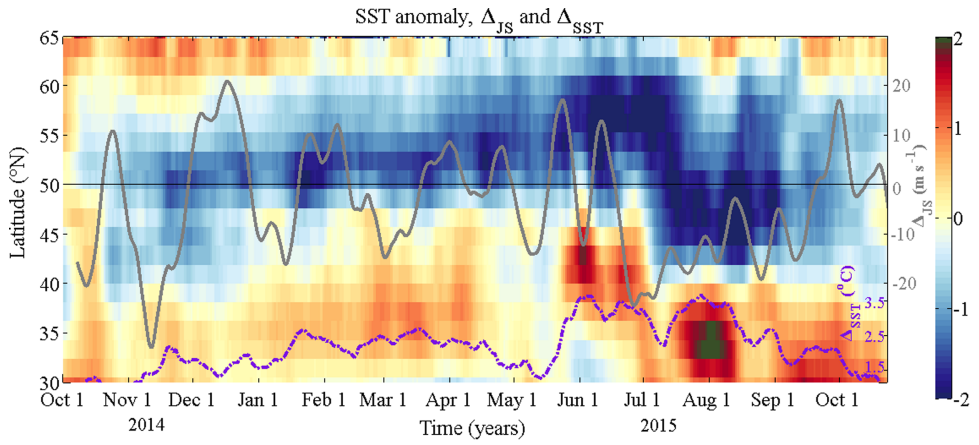

Figure 4. Hovmöller diagram of 2015 daily SST anomalies (in °C) averaged over 40–20°W (coloured field). Overlaid is the Jet Stream displacement measure (Δ_{JS}) represented with a solid grey line and smoothed using a 10-day running mean. Also shown is the difference in between the Southern Band (SB, 35–50°N) maximum SST and Northern Band (NB, 50–65°N) minimum SST (Δ_{SST}, purple dash-dot line).

deviation from the mean of 1.5 STD higher and for the summers 1994 and 1992 the deviations are 1.6 and 1.2 STD, respectively. These results show that 2015 was the most extreme central European heat wave in the 1980–2015 period considered. Moreover, using a gridded version (E-OBS 11.0) of the European Climate Assessment & Data (Haylock *et al* 2008), ECA&D, www.ecad.eu), Russo *et al* 2015 also showed that the summer of 2015 was the most extreme heat wave recorded in parts of central/eastern Europe and was classified within the top ten most extreme European heat waves since 1950.

Could this heat wave have been driven in part by the cold ocean temperature anomaly that preceded it? Previous model and observation based studies suggest that atmospheric circulation changes can develop in response to SST anomalies (Walin 1982, Sutton and Mathieu 2002, Nakamura *et al* 2005, Smeed *et al* 2014). To explore whether this is the case in 2015 we compare the daily SST field evolution to the timing of shifts in the position of the atmospheric Jet Stream (JS). The SST anomaly develops through winter 2014–15 and amplifies through spring into early summer preceding the onset of the heat wave (figure 4).

In order to estimate the strength of the JS shift, we define a measure of the southward JS displacement that captures the difference in high level (300 mb) wind speed between adjacent latitude bands north and south of 50°N: a northern band (NB, 50–65°N) and a southern band (SB, 35–50°N), in each case for the longitude range 50–10°W. This parameter indicates whether the JS is predominantly located to the north or south in the North Atlantic and is calculated as the difference in the mean zonal 300 mb wind speed (u_{300}) between the two bands:

$$\Delta_{JS} = \textbf{Mean } \mathbf{u}_{300NB} - \textbf{Mean } \mathbf{u}_{300SB}. \quad (2)$$

If the winds are stronger in the north than the south, Δ_{JS} takes positive values (up to 30 m s^{-1}). The value of Δ_{JS} becomes negative if the JS has been displaced into the southern band. Six-hourly values of Δ_{JS} have been calculated and smoothed with a 55-point Parzen filter to produce the time series shown on figure 4. In late June, Δ_{JS} undergoes a clear shift from a highly variable state, with no persistent positive or negative values, to a persistent state of negative values indicating a southward displacement of the JS (figure 4). This displacement is preceded by a strengthening of the meridional SST gradient in early June suggesting that the SST gradient increase leads the southward JS deflection by several weeks. This is demonstrated further by the purple line on figure 4, which shows the difference between the maximum warm anomaly in the southern band and the minimum cold anomaly in the northern band (called Δ_{SST}) rising sharply from mid-May to a maximum in the first week of June. The lagged response of the JS position to the strong meridional SST gradient indicates a potential role for the ocean in steering the JS position although further model experiments are required to confirm this suggestion. Δ_{JS} remains negative until September indicating that the JS is displaced southwards throughout much of the summer. From mid-July to the beginning of September, the most pronounced cold SST anomalies are located further southwards (at about 47°N rather than 57°N previously) which is consistent with a response of the ocean to the southward shift in the JS.

The 2015 heat wave results open an interesting route for research into whether Atlantic temperature anomalies have also contributed more generally to extreme European heat waves that have occurred in the last decades (figure 1(c) shows the timing of these heat waves). Past analyses have considered the role played by Mediterranean SST anomalies coinciding with specific heat waves (Xoplaki *et al* 2003, Feudale and Shukla 2011a, 2011b). We find a potential role for North Atlantic Ocean SSTs as a precursor of European

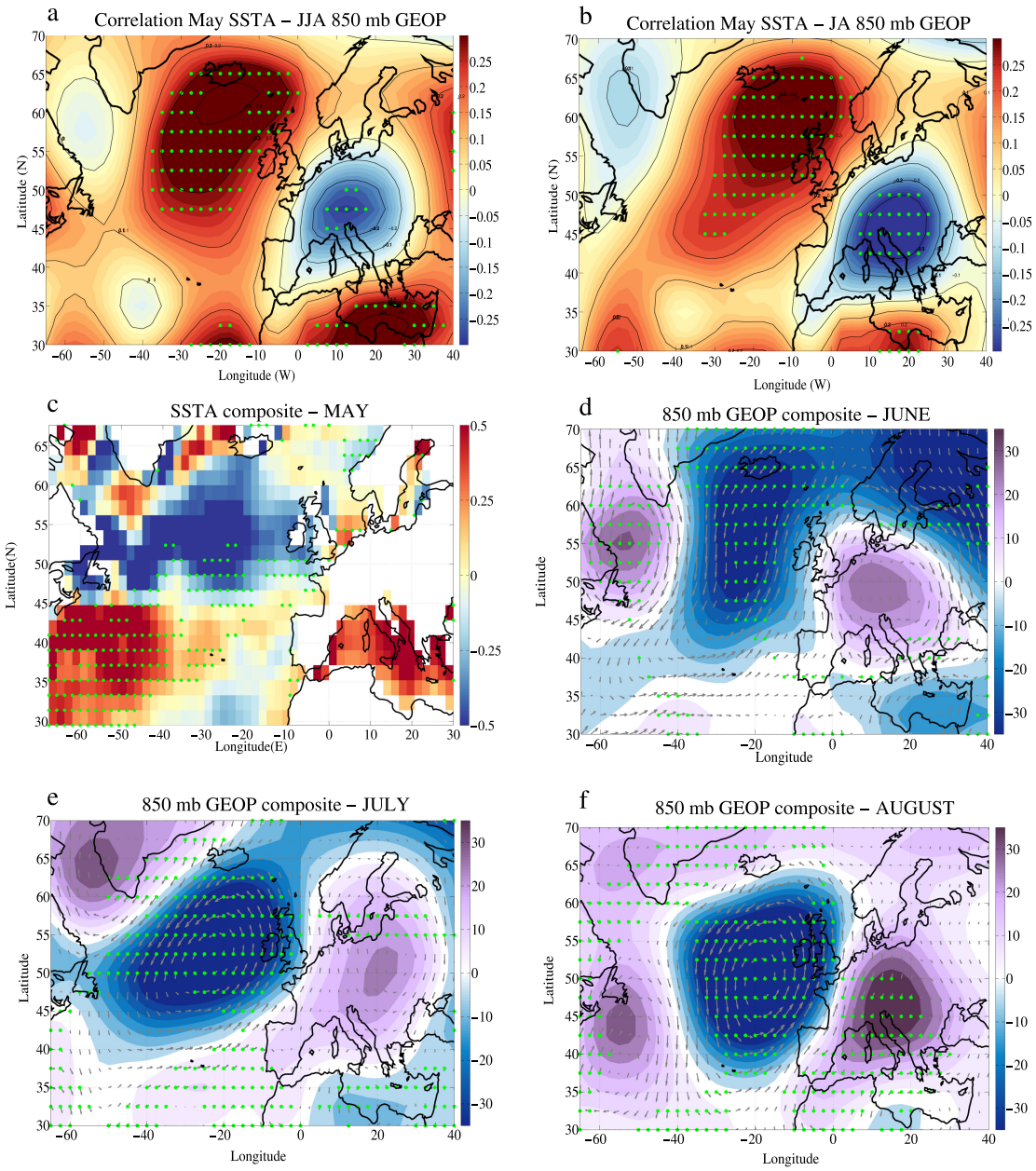

Figure 5. (a) Correlation between May SST anomaly averaged over the North Atlantic box (defined in figure 1(a)) and June–July–August (JJA) 850 mb geopotential height (GEOP) anomaly (in m) from 1980 to 2015, (b) as (a) but showing the correlation between May SST and July–August GEOP anomaly. (c)–(f) Composite mean fields determined for the set of 1980–2015 Central European heat waves (1992, 1994, 2003, 2012, 2015) of (c) May SST anomaly (in °C) and (d)–(f) 850 mb geopotential height anomaly (in m) for (d) June, (e) July and (f) August. The green dotted areas show the 95% significance level calculated using a Monte Carlo method.

heat waves using a lagged correlation analysis between May SST for the North Atlantic box (defined in figure 1(a)) and June–July–August averaged 850 mb height anomaly for all years from 1948–2015 (figure 5(a)).

Geopotential height over central Europe in summer (JJA) is significantly anti-correlated with the precursor SST field in May. The calculation has been repeated for mid-late summer by omitting June from the calculation and this reveals an intensification of the lagged correlation pattern (figure 5(b)). Note that in a previous study that considered the JJA SST field coincident with heat wave occurrence (Della-Marta *et al* 2007) an east–west dipole pattern was found with a different spatial structure from the one we find here for the precursor May SST field.

To further examine the lagged relationship between European heat waves and North Atlantic Ocean temperatures, we carry out a composite analysis of Atlantic SST anomalies in May and 850 mb geopotential height in June, July and August for the five leading summer European heat waves (figures 5(c)–(f)).

These five hottest summers were selected from the time series of maximum temperature (Tmax) and correspond to the years: 1992, 1994, 2003, 2012 and 2015. They were selected as the years for which the averaged

JJA European temperatures were above a one STD threshold (figure 1(c)). The European region used to estimate these heat waves is shown in figure 1(a) (right box). A Monte-Carlo method (e.g. Duchez *et al* 2015) was used to determine the significance levels of the signals in composite maps produced by averaging over the five hottest summers (figure 5). The significance level was calculated from the distribution of composite values obtained by repeated (1000 times) random selection of five summers (with replacement) during the period 1948–2015.

A cold anomaly is present in May (figure 5(c)) in conjunction and associated with a co-located low-pressure and an accompanying high-pressure anomaly over Europe in subsequent months June–August (figures 5(d)–(f)). Thus, a coherent picture emerges, from both the general lagged correlation analysis and the targeted composite study, of cold North Atlantic Ocean surface temperatures preceding the atmospheric circulation anomalies that lead to heat waves over Europe.

Note that this composite analysis has also been performed for cold summers (not shown) and although the ocean temperature anomalies are anticorrelated with Tmax above Central Europe (figures 5(a) and (b)), no warm summer anomaly in the southeast subpolar gyre is associated with these cold summers. This shows that the anticorrelation between SST and Tmax is mainly due to the processes happening during warm summers (i.e. the anomaly patterns coinciding with cold summers are not the inverse of the warm summers). Finally we also note that lagged correlations and composites described in here do not establish a causal link between the cold anomaly and European summer extreme temperatures but do show a significant lagged relationship between these two phenomena which requires a follow-on model study to confirm causality and the details of the mechanism involved.

5. Discussion and conclusions

The main focus of our study has been two climate events that occurred in 2015: exceptionally cold North Atlantic Ocean surface temperatures and a severe European summer heat wave, and the potential relationship between them. We have identified the causes of the cold ocean temperatures by observation based analysis of the range of possible drivers involved, including surface heat loss, ocean heat content and wind driven upwelling. The primary drivers are extreme ocean heat loss driven by atmospheric circulation changes in the preceding two winters combined with the re-emergence of cold ocean water masses.

We have also examined whether the cold ocean temperatures may have contributed to the development of the 2015 heat wave. In this case we have not been able to establish causality, as that would require a complex model analysis that considers the various possible factors advanced previously as potential drivers (including soil moisture, precipitation and Tropical Atlantic atmospheric warming) in addition to the cold ocean precursor. Nevertheless, our results have established that similar cold Atlantic anomalies were present prior to the onset of the most extreme European heat waves back to 1980 indicating that it is a common factor in their development. Furthermore, in the case of 2015, we suggest that the ocean anomaly, and the resulting strong meridional SST gradient could have initiated a propagating Rossby wave train causing a stationary Jet Stream position that favoured the development of high pressure and temperature extremes over Central Europe during the heat wave. However, this is still a hypothesis to be tested.

Our study calls for an urgent assessment of the impact of ocean drivers on major European summer temperature extremes in order to fully elucidate the driving mechanisms involved and consequently provide better advance warning measures of these high societal impact events.

Acknowledgments

AD is beneficiary of an AXA Research Fund postdoctoral grant. JJ-MH, SAJ, JPG, and BS are supported by the UK Natural Environment Research Council (NERC) National Capability funding. AD is partly funded by the UK-China Research and Innovation Partnership Fund through the Met Office Climate Science for Service Partnership (CSSP) China as part of the Newton Fund. JJ-MH is partly funded by CSSP and the NERC project ODYSEA (grant number: NE/M006107/1). JPG is partly funded by the project DYNAMOC (grant number NE/M005097/1). GDM is supported by the NERC RAPID-WATCH programme. EFW was supported by a Leverhulme Research Fellowship. RM acknowledge the support of various NERC grants. DGE is supported by a NERC Studentship Award at the University of Southampton. DB is supported by a NERC grant NE/J020788/1. We also thank the three anonymous reviewers for their thoughtful comments that significantly helped to improve the manuscript.

References

Black E, Blackburn M, Harrison R G, Hoskins B J and Methven J 2004 Factors contributing to the summer 2003 European heatwave *RMETS* **59** 217–23

Boyer T P *et al* 2013 *World Ocean Database 2013—NOAA Atlas NESDIS 72* ed S Levitus and A V Mishonov, technical edn (Silver Spring, MD: National Oceanographic Data Center Ocean Climate Laboratory) (ftp://ftp.nodc.noaa.gov/pub/WOD/DOC/wod_intro.pdf)

Brayshaw D J, Hoskins B and Blackburn M 2011 The basic ingredients of the North Atlantic storm track. Part I: Land–sea contrast and orography *J. Atmos. Sci.* **66** 2539–58

Buchan J, Hirschi J J-M, Blaker A T and Sinha B 2014 North Atlantic SST anomalies and the cold North European weather events

of winter 2009/10 and December 2010 *Mon. Weather Rev.* **142** 922–32
Cassou C, Terray L and Phillips A S 2005 Tropical Atlantic influence on European heat waves *J. Clim.* **18** 2805–11
Dee D P *et al* 2011 The ERA-Interim reanalysis: configuration and performance of the data assimilation system *Q. J. R. Meteorol. Soc.* **137** 553–97
Della-Marta P M, Luterbacher J, von Weissenfluh H, Xoplaki E, Brunet M and Wanner H 2007 Summer heat waves over western Europe 1880–2003, their relationship to large-scale forcings and predictability *Clim. Dyn.* **29** 251–75
Deser C, Alexander M A, Xie S-P and Phillips A S 2010 Sea surface temperature variability: patterns and mechanisms *Annu. Rev. Mar. Sci.* **2** 115–43
Dong B, Sutton R T, Woollings T and Hodges K 2013 Variability of the North Atlantic summer storm track: mechanisms and impacts on European climate *Environ. Res. Lett.* **8** 034037
Drijfhout S, van Oldenborgh G J and Cimatoribus A 2012 Is a decline of AMOC causing the warming hole above the North Atlantic in observed and modeled warming patterns? *J. Clim.* **25** 8373–9
Duchez A, Courtois P, Hirschi J J-M, Harris E, Josey S, Kanzow T, Marsh R and Smeed D 2015 Potential for seasonal prediction of Atlantic sea surface temperatures using the RAPID array at 26°N *Clim. Dyn.* **46** 3351–70
Evans D G, Zika J D, Naveira Garabato A C and Nurser A J G 2014 The imprint of Southern Ocean overturning on seasonal water mass variability in Drake passage *J. Geophys. Res. Ocean.* **119** 7987–8010
Feudale L and Shukla J 2011a Influence of sea surface temperature on the European heat wave of 2003 summer: I. An observational study *Clim. Dyn.* **36** 1691–703
Feudale L and Shukla J 2011b Influence of sea surface temperature on the European heat wave of 2003 summer. Part II: a modeling study *Clim. Dyn.* **36** 1705–15
Fischer E M, Seneviratne S I, Vidale P L, Lüthi D and Schär C 2007 Soil moisture–atmosphere interactions during the 2003 European summer heat wave *J. Clim.* **20** 5081–99
Grist J P, Josey S A, Jacobs Z L, Marsh R, Sinha B and Sebille E V 2015 Extreme air–sea interaction over the North Atlantic subpolar gyre during the winter of 2013–14 and its sub-surface legacy *Clim. Dyn.* **46** 4027
Haylock M R, Hofstra N, Klein Tank A M G, Klok E J, Jones P D and New M 2008 A European daily high-resolution gridded data set of surface temperature and precipitation for 1950–2006 *J. Geophys. Res.* **113** D20119
Josey S A, Gulev S and Yu L 2013 Exchanges through the ocean surface *Ocean Circulation and Climate: A 21st Century Perspective* ed G Siedler, S Griffies, J Gould and J Church, vol 103 2nd edn (New York: Academic) pp 115–40
Kalnay E *et al* 1996 The NCEP/NCAR 40-year reanalysis project *Bull. Am. Meteorol. Soc.* **77** 437–71
Marshall J C, Williams R G and Nurser A J G 1993 Inferring the subduction rate and period over the North Atlantic *J. Phys. Oceanogr.* **23** 1315–29
McCarthy G, Haigh I, Hirschi J, Grist J and Smeed D 2015 Ocean impact on decadal Atlantic climate variability revealed by sea-level observations *Nature* **521** 508–10
Meehl G a and Tebaldi C 2004 More intense, more frequent, and longer lasting heat waves in the 21st century *Science* **305** 994–7
Nakamura M, Enomoto T and Yamane S 2005 A simulation study of the 2003 heatwave in Europe *J. Earth Simulator* **2** 55–69
Parker A and Ollier C D 2016 There is no real evidence for a diminishing trend of the Atlantic meridional overturning circulation *J. Ocean Eng. Sci.* **1** 30–5
Perkins S E 2015 A review on the scientific understanding of heatwaves—their measurement, driving mechanisms, and changes at the global scale *Atmos. Res.* **164–165** 242–67
Perkins S E and Alexander L V 2012 On the measurement of heat waves *J. Clim.* **26** 4500–17
Pond S and Pickard G L 1983 *Introductory Dynamical Oceanography* 2nd edn (Oxford: Butterworth-Heinemann)
Rahmstorf S, Box J E, Feulner G, Mann M E, Robinson A, Rutherford S and Schaffernicht E J 2015 Exceptional twentieth-century slowdown in Atlantic Ocean overturning circulation *Nat. Clim. Chang.* **5** 1–6
Roemmich D and Gilson J 2009 The 2004–2008 mean and annual cycle of temperature, salinity, and steric height in the global ocean from the Argo Program *Prog. Oceanogr.* **82** 81–100
Russo S, Sillmann J and Fischer E M 2015 Top ten European heatwaves since 1950 and their occur- rence in the future *Environ. Res. Lett.* **10** 124003
Smeed D a *et al* 2014 Observed decline of the Atlantic meridional overturning circulation 2004–2012 *Ocean Sci.* **10** 29–38
Stefanon M, D'Andrea F and Drobinski P 2012 Heatwave classification over Europe and the Mediterranean region *Environ. Res. Lett.* **7** 014023
Sutton R and Mathieu P-P 2002 Response of the atmosphere–ocean mixed-layer system to anomalous ocean heat-flux convergence *Q. J. R. Meteorol. Soc.* **128** 1259–75
Vallis G K 2006 *Atmospheric and Oceanic Fluid Dynamics* (Cambridge: Cambridge University Press) p 745
Vautard R, Honoré C, Beekmann M and Rouil L 2005 Simulation of ozone during the August 2003 heat wave and emission control scenarios *Atmos. Environ.* **39** 2957–67
Walin G 1982 On the relation between sea-surface heat flow and thermal circulation in the ocean *Tellus* **34** 187–95
Willis J K 2010 Can *in situ* floats and satellite altimeters detect long-term changes in Atlantic Ocean overturning *Geophys. Res. Lett.* **37** L06602
Xoplaki E, Gonzalez-Rouco J F, Luterbacher J and Wanner H 2003 Mediterranean summer air temperature variability and its connection to the large-scale atmospheric circulation and SSTs *Clim. Dyn.* **20** 723–39